Increase of nonlocal spin signal at high dc bias due to a redistribution of the injection current

X. J. Wang, H. Zou, and Y. Ji*
Department of Physics and Astronomy, University of Delaware, Newark, Delaware 19716, USA
(Received 10 November 2009; revised manuscript received 24 February 2010; published 15 March 2010)

The spin signals in nonlocal spin valves with 1.3 nm AlO_x layers as spin-injection and spin-detection interfaces have been measured as a function of the dc bias current through the injector. Increases of the spin signals have been observed in both polarities of the injection current, with magnitudes up to 81%. This is attributed to a redistribution of the injection current due to a nonlinear resistivity at a higher bias. The baseline of the spin signal varies as a function of the bias current as well, and it is consistent with the interpretation of current redistribution. A temperature dependence of the spin signals has been conducted to demonstrate that the 81% increase of spin signal cannot be accounted for by the Joule heating of the device.

DOI: 10.1103/PhysRevB.81.104409 PACS number(s): 85.75.−d

Nonlocal spin valve (NLSV) has been explored using both metallic materials[1–6] and semiconductor materials[7–9] for spin-injection and spin-detection experiments recently. The NLSV structures allow for the unambiguous detection of spin accumulation and accurate determination of spin-diffusion length and spin-injection polarization. A pure spin current without a net charge current is another distinct advantage of the NLSV structure because its low power dissipation is attractive to spintronic applications in ultrasmall devices. The lateral layout the NLSV facilitates the fabrication of multiterminal structures. New physics in the spin-injection and the spin-relaxation processes have been revealed in the NLSV system.[10–12]

The NLSV measurements are typically done using an alternating current (ac) for spin injection, and the ac nonlocal voltages are measured using lock-in technique. A direct current (dc) bias can also be superimposed on the injector to provide a dc spin current. The bias dependence of the spin signals is an important issue because some spintronic effects require a substantial dc spin current density. An example is the spin-transfer torque effect.[12,13] Therefore, it is of relevance to understand how the spin polarization varies at high injection current density. The dependence of the spin signal in NLSV upon a dc injection current has been previously studied by Valenzuela *et al.*[4] and ourselves.[14,15] Valenzuela *et al.*[4] reported a rapid decrease in spin signal as the bias voltage on the $FeCo/Al_2O_3/Al$ injection interface is increased. The Al_2O_3 layer was formed by natural oxidation on Al and the resistance of the junction was ~50 kΩ. It is interpreted as the variations in the density of states available for electron tunneling as the energy bands of the nonmagnetic and ferromagnetic materials are shifted relative to each other by the bias. We have previously reported a bias-dependent measurement in the Co/Cu NLSV structures with ohmic interfaces.[14] The measurements were complicated by a possible degradation of the sample by prolonged exposure to a high current density. But an increase of the spin signal was clearly observed. This is interpreted as a redistribution of the injection current at higher bias, which reduces the effective distance between the injector and detector. Later, we have fabricated NLSV structures with $Co/AlO_x/Cu$ injection and detection interfaces.[15] The AlO_x layer is ~2 nm thick and the *RA* (resistance-area) product ($<10\ \Omega\ \mu m^2$) is relatively low. We measured the spin signal as a function of bias current up to a modest current 1.0 mA at 4.2 K. The spin signal was essentially unchanged.

In this work, we report an increase of the spin signal up to 81% in a NLSV structure with $Co/AlO_x/Cu$ interfaces under a bias current up to 2.2 mA. The increase has been observed for both polarities of the current, albeit with different magnitudes. This result reinforces our previous interpretation[14] that a redistribution of the injection current occurs at the injection interface as the bias is increased. Unlike the ohmic Co/Cu interfaces, the redistribution of the current at the $Co/AlO_x/Cu$ interface is translated into an enhanced effective spin-injection polarization due to the higher resistance of the AlO_x interfaces compared to ohmic interfaces. We also note that the bias current used here (up to 2.2 mA) is higher than those (up to 1.0 mA) used in Ref. 15. The AlO_x layer in this work (1.3 nm for the device showing largest bias dependence) is thinner than the 2 nm AlO_x layers used in Ref. 15. These differences may contribute to the fact that this dramatic increase of spin signal was not observed in the device in Ref. 15.

The fabrication and measurements of Co/Cu NLSV structures with AlO_x barriers were discussed in Ref. 15. To gain a general understanding of the basic characteristics of our NLSV structures, it is helpful to look at a batch of NLSV devices fabricated on the same chip. Figure 1 illustrates a batch of three devices measured at room temperature as well as 4.2 K. A scanning electron microscope (SEM) picture of a similar (but not the same) device is shown in the inset of Fig. 1(a). The nominal thicknesses of Co, Cu, and AlO_x are 26 nm, 100 nm, and 2.6 nm, respectively. The thicknesses of AlO_x layers at the injection and the detection interfaces are the same. The widths of the Co injector and detector are 250 nm and 200 nm, respectively. The width of the Cu wire is 250 nm. The center-to-center separations L between Co injector and detector are 500, 600, and 800 nm for the three devices.

The measurements are carried out by using an ac current (I_{ac}) between 0.2 and 0.5 mA, and the value of R_s is defined as $R_s = V_s/I_{ac}$, where V_s is the nonlocal voltage measured by a lock-in amplifier. The value of R_s as a function of magnetic field H for a device with $L=500$ nm is shown in Fig. 1(a), with the room-temperature curve vertically shifted for clarity. The values of R_s switch between two distinct states $R_{\uparrow\uparrow}$ and $R_{\uparrow\downarrow}$, corresponding to parallel and antiparallel alignments of

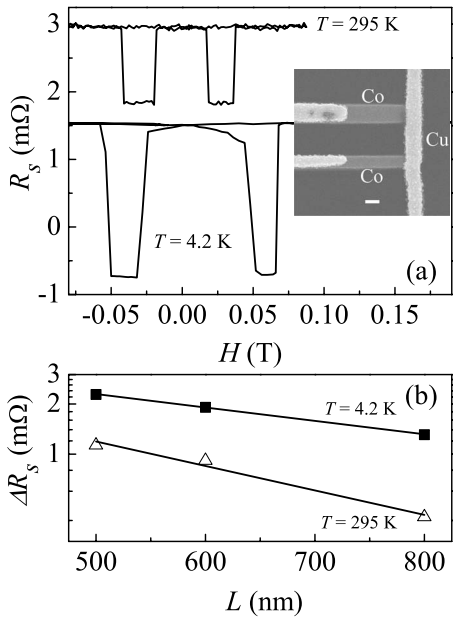

FIG. 1. Spin-signal measurements at 295 and 4.2 K for a batch of NLSV structures with 2.6-nm-thick AlO_x. (a) R_s versus H for a device with $L=500$ nm. The SEM picture of a similar device is shown in the inset. The scale bar represents 200 nm. (b) ΔR_s versus L for 4.2 K (solid squares) and 295 K (open triangles). The solid lines are fits using the ΔR_s formula in the text. The fitting yields $P=14\%$ and $\lambda_s=540$ nm at 4.2 K and $P=13\%$ and $\lambda_s=296$ nm at 295 K.

injector and detector magnetizations, respectively. The spin signal is defined as the difference: $\Delta R_s=R_{\uparrow\uparrow}-R_{\uparrow\downarrow}$. At room temperature $\Delta R_s=1.13$ mΩ and at 4.2 K $\Delta R_s=2.28$ mΩ. The ΔR_s versus L plot for both temperatures is shown in Fig. 1(b). Fitting the data using formula $\Delta R_s=P_1P_2\rho\lambda_s/Ae^{-L/\lambda_s}$,[16] we obtained spin polarization $P=P_1=P_2=13\%$ at room temperatures and $P=14\%$ at 4.2 K. The spin-diffusion length of Cu is $\lambda_s=296$ nm at room temperature and $\lambda_s=540$ nm at 4.2 K. P_1 and P_2 are the interface spin polarizations of the Co injector and the detector. Since the two electrodes are made of the same material and with similar dimensions, we assume $P_1=P_2$. The resistivity ρ of Cu is 1.33 $\mu\Omega$ cm at 4.2 K and 3.33 $\mu\Omega$ cm at room temperature, measured *in situ* in the NLSV structures.

The bias-dependent measurements have been performed for a number of NLSV devices. A device with 1.3-nm-thick AlO_x at the Co/Cu injection and detection interfaces yields the most dramatic bias-dependent effect. The thickness of the Co electrodes for this device is 23 nm. The value of L is 500 nm. All other dimension parameters are the same as the batch of devices shown in Fig. 1.

Figure 2(a) illustrates the R_s versus H curve at zero dc bias, measured at 4.2 K, showing a spin signal $\Delta R_s=1.04$ mΩ. The room-temperature measurement yields almost the same value of ΔR_s. For this device, there are no other devices fabricated on the same chip to establish a ΔR_s versus L curve and determine P and λ_s. However, another set of our experimental data indicates that devices with 18 nm Co electrodes and 1.3 nm AlO_x give $P\sim12\%$ at room temperature. Therefore, we assume $P\sim13\%$ at 4.2 K for the

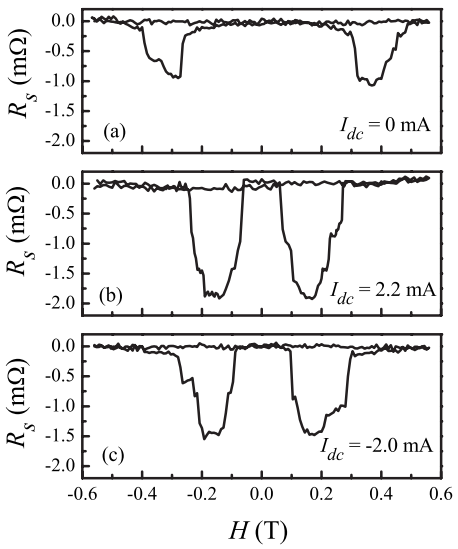

FIG. 2. The bias-dependent R_s versus H measurements for a NLSV structure with 1.3-nm-thick AlO_x. The curves are vertically shifted so that $R_{\uparrow\uparrow}=0$ for clarity. The dc bias currents are (a) 0 mA, (b) +2.2 mA, and (c) −2.0 mA.

current device exhibiting large bias dependence. We deduce $\lambda_s\sim400$ nm at 4.2 K and $\lambda_s\sim300$ nm at room temperature for this device.

The dc bias-dependent measurements are carried out with dc bias currents up to 2.2 mA in both polarities. In the positive polarity, the electrons flow from the Cu into the Co injector. The spin signal gradually increases as the bias is increased. The R_s as a function of H curves for $I_{dc}=+2.2$ mA and $I_{dc}=-2.0$ mA are shown in Figs. 2(b) and 2(c). The spin signals are 1.89 mΩ for +2.2 mA and 1.53 mΩ for −2.0 mA. It can be clearly noticed that the switching fields are different at higher bias compared to zero bias. This is due to the temperature increase resulting from the Joule heating of the bias current. The spin signal as a function of the bias measured at 4.2 K is plotted in Fig. 3(a). The spin signal increases in both polarities of the bias current. This curve is well reproducible for repeated measurements at various bias values, indicating the damage to the structure due to high current density is minimal. The asymmetry of the spin signal between the two polarities could be due to a change in density of states available for spin-dependent electron tunneling when the two bands are shifted on the energy scale by a bias voltage, as explained by Valenzuela *et al.*[4]

It is a legitimate question whether this increase of spin signal is a result of the increased temperature of the device under a large bias current. Kimura *et al.*[17] reported an anomalous temperature dependence of spin signals with the maximum value of spin signals located around 40 K. We perform temperature-dependent measurements under zero dc bias between 4 and 70 K, as shown in Fig. 3(b). There are slight variations in the spin signal even at the same nominal temperature, possibly due to some temperature instability of the sample stage. The values plotted in Fig. 3(b) are the largest zero-bias spin signals observed at each temperature. The highest spin signal we observe in the entire temperature-

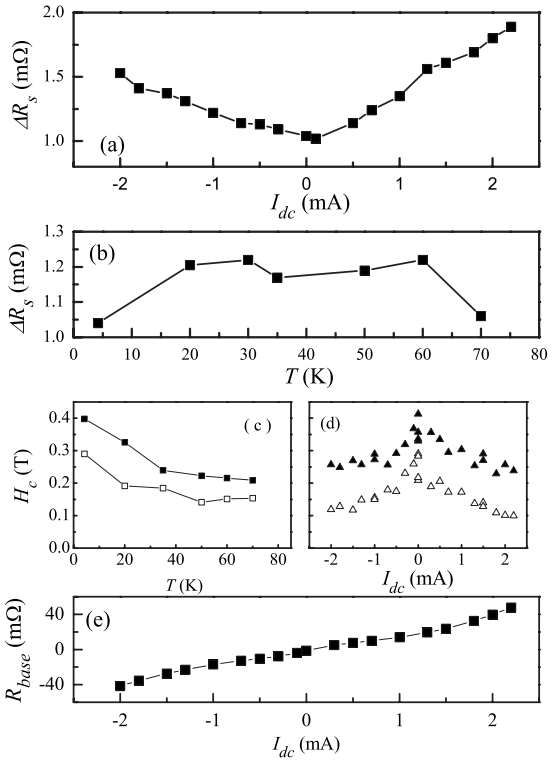

FIG. 3. A summary of various measurements for the device with 1.3 nm AlO_x, of which the bias-dependent measurements are shown in Fig. 2. (a) Spin signal as a function of the dc bias current measured at 4.2 K. (b) Spin signal as a function of temperature. (c) Coercive fields of the injector (H_{c1}, open squares) and detector (H_{c2}, solid squares) as a function of temperature. (d) H_{c1} (open triangles for the injector) and H_{c2} (solid triangles for the detector) as a function of bias current. (e) The baseline of the spin signal as a function of dc bias current.

dependent measurement is 1.22 mΩ, still much lower than the highest spin signal we observe in the bias-dependent measurements. In the results by Kimura *et al.*,[17] the maximum percentage increase of the spin signals in the temperature-dependent measurements is also much smaller than the maximum percentage increase (81%) in our bias-dependent measurement. Therefore, we conclude that the bias dependence cannot be accounted for by the temperature increase induced by Joule heating.

In addition, we investigated the switching fields as a function of the temperature. The coercive fields of the two electrodes (H_{c1} for the injector and H_{c2} for the detector) are plotted as a function of temperature in Fig. 3(c). As expected, both H_{c1} and H_{c2} decrease when the temperature is increased. As a comparison, H_{c1} and H_{c2} as a function of the bias current is plotted Fig. 3(d). The average temperature of the device will be discussed soon. There is a similar decrease in both coercive fields as the bias is increased, due to the Joule heating from the bias current. A comparison between Figs. 3(c) and 3(d) allows for a rough estimate of the device temperature under 2 mA bias. The value of H_{c1} (injector) at ±2 mA [Fig. 3(d)] is lower than H_{c1} at 70 K [Fig. 3(c)], indicating the temperature of injector under 2 mA bias is higher than 70 K. The value of H_{c2} (detector) at ±2 mA

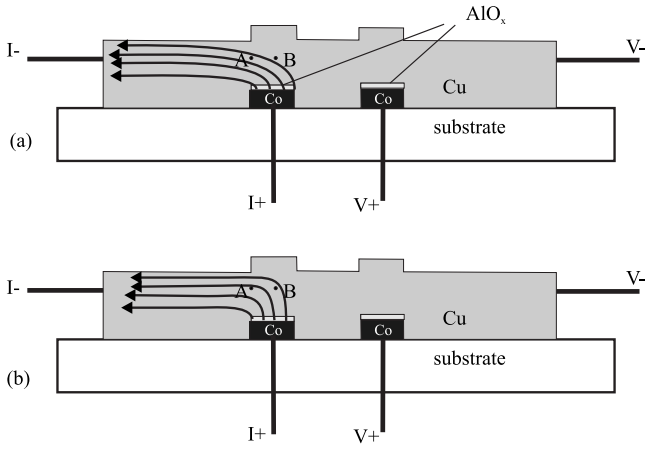

FIG. 4. (a) A schematic of current distribution in the NLSV structure at zero bias. (b) Current distribution at higher bias.

[Fig. 3(d)] is higher than the value of H_{c2} at 70 K [Fig. 3(c)], indicating the temperature of detector under 2 mA bias is lower than 70 K. This is a reasonable result since the bias current passes through the injector but not the detector, and thus a temperature difference is expected. It is also reasonable to say that the average temperature of the device under 2 mA bias is ~70 K, which is on the downward slope of the temperature dependent curve of the spin signal, shown in Fig. 3(b). However, in Fig. 3(a), the spin signals continue to increase up to 2 mA bias without showing signs of a decreasing trend. This further reinforces the conclusion that the increase of spin signal at high bias cannot the explained by temperature effects.

Figure 3(e) shows the baseline of the spin signal as a function of the bias. The baseline is defined as $R_{base}=R_{\uparrow\uparrow}+R_{\uparrow\downarrow}/2$. In principle, the baseline for an ideal one-dimensional nonlocal spin valve should be zero. But in most experiments, this value is nonzero. Johnson and Silsbee[18] provided a calculation to demonstrate that the complex current distribution in the actual three-dimensional device is one of the causes of the nonzero baseline. In Fig. 3(e), the baseline varies as a function of the bias current, indicating that the current distribution varies as the bias is increased. This will be further discussed later.

We interpret the increased spin signal under a bias current, as shown in Fig. 3(a), as a redistribution of the injection current at the $Co/AlO_x/Cu$ injection interface. The current density through the NLSV device is high. For a 2.0 mA bias current, the current density is $\sim 4\times 10^6$ A/cm^2 across the $Co/AlO_x/Cu$ interface and $\sim 9\times 10^6$ A/cm^2 through the Cu wire. Figure 4 provides a schematic that illustrates our understanding of the current redistribution process. A cross-sectional view is shown for the NLSV structure. Figure 4(a) illustrates the current distribution under zero dc bias. The solid lines with arrows indicate the current directions. The AlO_x at the interface provides a relatively large resistance compared to ohmic interfaces, and thus the current is essentially perpendicular to the interface. The current is directed to the left side of the Cu stripe, and the Cu layer is fairly thick (100 nm). Thus the current lines gradually turn from the perpendicular to the interface toward parallel to the interface

as it enters the copper wire. Therefore near the $Co/AlO_x/Cu$ interface on the Cu side, there is a region with highly inhomogeneous current density. Note the two representative locations A and B in Fig. 4(a). There is a fairly high current density at point A but much lower current density at point B.

As the bias current is increased, the current density increases in the Cu wire. Initially the current distribution remains the same as shown in Fig. 4(a) because the resistivity of the Cu remains a constant at low bias obeying the Ohm's law. When the current density is large enough ($>10^6$ A/cm^2), the resistivity gradually increases as a function of the bias current density. This has been seen in many nanoscale systems[13,19,20] such as point contacts and nanopillars, and is attributed to phonon scattering and local heating. Since the current density is higher at A compared to B. The resistivity at point A increases faster than the resistivity at point B. Therefore, the current will be diverted from point A toward point B because a path with a smaller resistance is favored for electric current. In this manner, the current redistributes and it is shown schematically in Fig. 4(b). In this configuration, the current is more perpendicular to the interface, compared to the zero-bias current distribution shown in Fig. 4(a). This gives a higher effective injection polarization. In the current-perpendicular-to-plane giant magnetoresistance (GMR) structures, superconducting layers have been made to direct the current perpendicular to the interfaces to ensure large GMR values.[21] We have previously estimated $P_1=P_2\sim 13\%$ for this NLSV device. The current redistribution does not affect detector polarization P_2. Therefore, an 81% increase of spin signal results in an effective spin-injection polarization (P_1) of ~23%, which is still lower than the intrinsic bulk spin polarization (~45%) of Co.[22]

Comparing with Fig. 4(a), we noticed in Fig. 4(b) that in the positive bias, there is a larger upward component of the current perpendicular to the interface. This will enable a larger positive voltage drop between the V+ (connected to Co detector) and V− (connected to right side of Cu) terminals in the positive bias because the V+ is located lower than V−. In a similar fashion, a larger negative voltage will be induced between V+ and V− in the negative bias. Therefore, the baseline will increase at positive bias and decrease at negative bias. This is indeed what is observed and shown in Fig. 3(e).

The bias-dependent measurements of the spin signal have been conducted for a few other devices. The thickness of AlO_x at the injection and the detection interfaces in these devices ranges from 0.8 to 2.6 nm, and the thickness of Co ranges from 18 to 35 nm. The bias dependence increases of the spin signals are found to be between 0% and 20%. It is not straightforward to establish a correlation between the bias-dependent increase of the spin signal and the thickness of AlO_x or Co. Other factors, such as the morphology and the microstructure of the interfaces, may also play a role in addition to nominal geometrical factors of the structures. The precise conditions for this effect are subject to further studies. We note that the resistance values of injection and detection junctions could also influence the spin signals[23] and this is subject to further studies as well. The $Co/AlO_x/Cu$ interface should be useful for realizing spin-transfer effects in NLSV because the injection polarization is substantial and there is no decrease in polarization at higher bias.

In conclusion, we have investigated the dependence of the spin signal upon a dc bias current in a Co/Cu nonlocal spin valve with 1.3 nm AlO_x at injection and detection interfaces. The spin signal increases for both polarities of the current. The magnitude of the increase is 81% for 2.2 mA in the positive polarity (electrons going from Cu to Co), and 47% for 2.0 mA in the negative polarity (electrons going from Co to Cu). These values cannot be accounted for by the Joule heating of the bias current. We interpret the increase of the spin signal under dc bias as a redistribution of the injection current at high current density.

The authors acknowledge use of University of Maryland NanoCenter facilities. This work has been supported by DOE under Grant No. DE-FG02-07ER46374.

*Corresponding author; yji@physics.udel.edu

[1] M. Johnson and R. H. Silsbee, Phys. Rev. Lett. **55**, 1790 (1985).
[2] F. J. Jedema, A. T. Filip, and B. J. van Wees, Nature (London) **410**, 345 (2001).
[3] T. Kimura, J. Hamrle, Y. Otani, K. Tsukagoshi, and Y. Aoyagi, Appl. Phys. Lett. **85**, 3501 (2004).
[4] S. O. Valenzuela, D. J. Monsma, C. M. Marcus, V. Narayanamurti, and M. Tinkham, Phys. Rev. Lett. **94**, 196601 (2005).
[5] Y. Ji, A. Hoffmann, J. S. Jiang, and S. D. Bader, Appl. Phys. Lett. **85**, 6218 (2004).
[6] S. Garzon, I. Zutic, and R. A. Webb, Phys. Rev. Lett. **94**, 176601 (2005).
[7] O. M. J. van 't Erve, A. T. Hanbicki, M. Holub, C. H. Li, C. Awo-Affouda, P. E. Thompson, and B. T. Jonker, Appl. Phys. Lett. **91**, 212109 (2007).
[8] X. Lou, C. Adelmann, S. A. Crooker, E. S. Garlid, J. Zhang, K. S. Madhukar Reddy, S. D. Flexner, C. J. Palmstrom, and P. A. Crowell, Nat. Phys. **3**, 197 (2007).
[9] D. Saha, M. Holub, and P. Bhattacharya, Appl. Phys. Lett. **91**, 072513 (2007).
[10] S. O. Valenzuela and M. Tinkham, Nature (London) **442**, 176 (2006).
[11] T. Kimura, Y. Otani, T. Sato, S. Takahashi, and S. Maekawa, Phys. Rev. Lett. **98**, 156601 (2007).
[12] T. Yang, T. Kimura, and Y. Otani, Nat. Phys. **4**, 851 (2008).
[13] J. A. Katine, F. J. Albert, R. A. Buhrman, E. B. Myers, and D. C. Ralph, Phys. Rev. Lett. **84**, 3149 (2000).
[14] X. J. Wang, H. Zou, L. E. Ocola, R. Divan, and Y. Ji, J. Appl. Phys. **105**, 093907 (2009).
[15] X. J. Wang, H. Zou, L. E. Ocola, and Y. Ji, Appl. Phys. Lett. **95**, 022519 (2009).
[16] M. Johnson, Phys. Rev. Lett. **70**, 2142 (1993).
[17] T. Kimura, T. Sato, and Y. Otani, Phys. Rev. Lett. **100**, 066602 (2008).

[18] M. Johnson and R. H. Silsbee, Phys. Rev. B **76**, 153107 (2007).
[19] E. B. Myers, D. C. Ralph, J. A. Katine, R. N. Louie, and R. A. Buhrman, Science **285**, 867 (1999).
[20] Y. Ji, C. L. Chien, and M. D. Stiles, Phys. Rev. Lett. **90**, 106601 (2003).
[21] Q. Yang, P. Holody, R. Loloee, L. L. Henry, W. P. Pratt, Jr., P. A. Schroeder, and J. Bass, Phys. Rev. B **51**, 3226 (1995).
[22] G. J. Strijkers, Y. Ji, F. Y. Yang, C. L. Chien, and J. M. Byers, Phys. Rev. B **63**, 104510 (2001).
[23] A. Fert and H. Jaffres, Phys. Rev. B **64**, 184420 (2001).